Available online at www.sciencedirect.com

ScienceDirect

Procedia CIRP 93 (2020) 568–574

www.elsevier.com/locate/procedia

53rd CIRP Conference on Manufacturing Systems

Using finite element analysis to develop a digital twin of a manufacturing bending operation

E.P.Hinchy[a,c],* C. Carcagno[b], N.P. O'Dowd[a,c,d], C.T. McCarthy[a,c,d]

[a]*Confirm Smart Manufacturing Research Centre, Ireland*
[b]*Sigma Clermont, 63170 Aubière, France*
[c]*Bernal Institute, University of Limerick, Ireland*
[d]*School of Engineering, University of Limerick, Ireland*

* Corresponding author. Tel.: +353 61 202136. *E-mail address: Eoin.Hinchy@ul.ie*

Abstract

In smart manufacturing, a digital twin is the virtual counterpart of a physical manufacturing system and can be considered as having three elements: machine, product and process. To demonstrate this concept, a physical manufacturing testbed was developed which bends metal into V-brackets alongside a digital twin counterpart consisting of the three elements. The process digital twin uses finite element modelling to predict product stress during the bending operation, and the residual stress and bend angle post-bending. The bend angles predicted by the process digital-twin were within 0.5° and 3° of the physical product for two different test scenarios.

Keywords: Digital Twin; Smart Manufacturing; Finite Element Modelling;

1. Introduction

Smart Manufacturing is a multidisciplinary area, covering business, computer science, electrical, mechanical, and process engineering [1]. Also known as the fourth industrial revolution and Industry 4.0, smart manufacturing sees the convergence of information and communication technology (ICT) with manufacturing technologies, for improved efficiency and productivity with reduced time to market [2,3]. One of the key areas of smart manufacturing is cyber physical systems (CPSs), which relates to the integration of the physical and cyber worlds [1]. A CPS can enhance product design, manufacturing production systems, as well as product performance during lifecycle [4]. In terms of manufacturing, these systems are often referred to cyber-physical productions systems (CPPSs), which is an applied form of CPS [5].

Digital twin technology has gained extensive attention in recent times, both within industry and academia [6]. In manufacturing, a digital twin can be considered as the cyber element of a CPPS [6]. There is no single scientific definition of digital twin, however, a common definition is that a digital twin is a "Digital representation of a real world object with focus on the object itself" [7]. The role of digital twins in manufacturing has evolved since the initial concept was developed. Early research on digital twins used this technology to monitor health and maintenance of physical manufacturing equipment. However, this technology is more recently being used to mirror physical entities, predicting performance and behavior under different conditions [8]. High-fidelity digital models can be used to virtually reproduce physical geometries, properties and behaviors [9]. Real-world sensor data can then be combined with these models and simulations to improve the physical manufacturing process [10,11]. For example, a digital twin of a physical manufacturing operation can be used to predict, analyze and optimize the process in the virtual environment. Once optimized in the virtual world, the optimized solution can be applied to the real world physical process – adding business value [10].

10.1016/j.procir.2020.03.031

Traditional manufacturing processes can be considered as having three primary elements. The first element is the manufacturing machine, which is doing the manufacturing operation. The second element is the product, the component to which the manufacturing machine is adding value. The final element is the physical process that the machine is carrying out on the product. Each of these three elements should be represented by a digital twin component.

A number of authors have reported works for individual digital twin elements. However, the integration of the machine, product and process digital twin elements is yet to be reported. For example, object orientated modelling has been reported for a machining process, where the machine and process have been modelled in the endeavor to create a digital twin [12]. There has also been interest in developing high-fidelity process models for additive manufacturing processes with a view to developing a digital twin [13]. Some of these process models predict product microstructures [14], while others predict residual stress and distortion in the final product [15].

One of the major benefits of digital twin technology is the ability to make predictions about the expected product behavior [16]. Motivated by this, this paper presents a novel approach for manufacturing-based digital twins, combining digital twin elements for the *machine*, *product* and *process*. A physical testbed has been developed to demonstrate this approach, which has been designed to V-bend metallic materials. This paper focuses on reporting the process digital twin element, which uses a finite element model (FEM) to gain insights and make predictions about the bending process and product outcomes.

This paper is structured as follows: Section 2 outlines the materials and methods used for experimentation and modelling. Section 3 presents the results from both modelling and experimental tests while Section 4 discusses these results. Finally, Section 5 presents the concluding comments, as well as future research opportunities.

2. Materials and Methods

Bending was selected as a manufacturing operation for the test bed, as it is a common manufacturing process in aerospace and automotive industries which can easily be interpreted. The physical twin is comprised of three elements, the machine, the product, and the process. The bending machine, see Fig. 1, uses a pair of high-torque stepper motors to move a V-press relative to the static V-die, while a load cell is used to measure load during the bending cycle. The V-press displacement has a step resolution of 0.5 mm, while the repeatability of the displacement was determined using a Vernier calipers to be +/- 0.2 mm. The system is controlled using an IoT-enabled Raspberry Pi model 3B+, which is capable of wirelessly transmitting sensor data via OPC-UA protocol. A number of bespoke components such as button enclosures and brackets were designed using Solidworks and 3D printed with polylactic acid (PLA) plastic using a Prusa i3 Mk3 fused filament fabrication 3D printer. The machine digital twin element consisted of a 3D CAD model designed using Solidworks, see Fig. 1, which was capable of simulating the kinematic movements of the V-press relative to the die. The machine digital twin element also includes the operational code, as well as machine operational history information such as the number of bending cycles completed.

The physical product being manufactured is a metallic bracket made from aluminum 2024 T3 series. This material was selected as it is strong, lightweight, is used in the aerospace industry, and has previously been modeled in other bending applications [17], [18]. Elastic and dimensional details of Al2024 T3 can be seen in Table 1, while the plastic properties of this material is plotted in Fig. A.1 in Appendix A. The product digital twin element consists of a database of product features, including material type, material properties, product dimensions and product condition (i.e. pre- or post-bending).

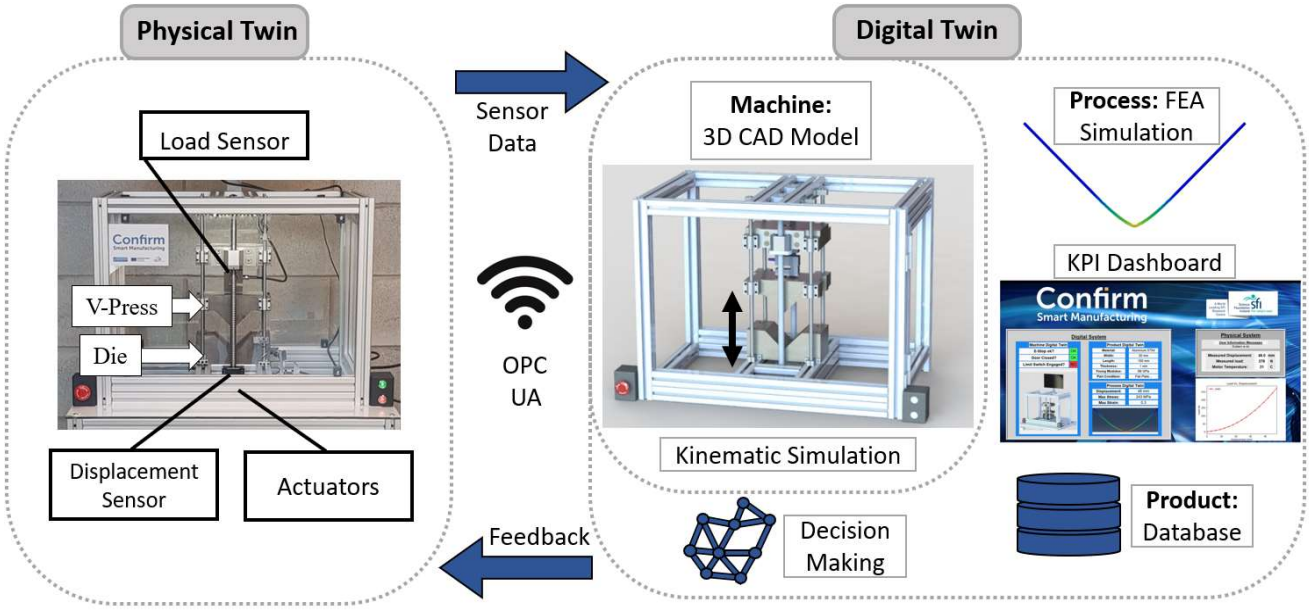

Fig. 1 Schematic illustrating integration of physical system (left) and digital system (right)

Table 1: Elastic and dimensional material properties of Al2024 T3

Material	Young's Modulus (GPa)	Poisson's Ratio	Length (mm)	Width (mm)	Thickness (mm)
Al 2024 T3	73.626	0.33	150	30	1.27

The physical process bends an initially flat strip of Al2024 placed across the die opening into a V-shape. The start button initiates the bending cycle and the cross-head moves downward by a prescribed distance, bending the metallic strip between the V-press and die. There is a two-second hold, and the crosshead then lifts the V-press to the home position.

The process digital twin is a non-linear 2D finite element model (FEM) implemented using Abaqus®. The process digital twin predicts the final bend angle, the stress in the product during bending and the residual stress after manufacture. This FEM contains three parts: the V-press, the die and the plate (product). The former two parts are rigid bodies meshed with 2-node R2D2 elements. The geometry of the press and die are shown in Fig. 2. The plate is modelled as a deformable part partitioned in three different sub-parts allowing a different mesh density within the plate – a technique also employed by Chan et al., [17], for FEM of springback of V-bending aluminum sheet. The purpose of the mesh partition is to increase mesh density in the location where the V-press meets the plate. Eight node (quadratic) plane stress elements (CPS8) were used for the plate.

A frictional slip tolerance of 0.005 and a coefficient of friction of 0.01 were used for the boundary conditions between the V-press and workpiece, and the workpiece and die. The maximum displacement of the V-press is 48.5 mm from the point of touching the specimen until the point when the press fully mates with the die. Two bending test scenarios were performed during this study. The first scenario involved modelling the bending process to a V-press displacement of 30 mm. For the second scenario, a V-press displacement of 45 mm was examined. For each of these two scenarios, physical tests were conducted using the metal bending test bed. These tests involved bending ten specimens for each scenario, where the final bend angle of each specimen was measured using ImageJ

3. Results

The fundamental idea behind digital twin technology is to add value to any manufacturing system using cyber physical systems through process predictions and optimization. The development of an FEM-based process digital twin is one such method for predicting manufacturing outcomes.

3.1 Process digital twin: 30 mm displacement

For the first FEM-based process digital twin, the V-press travelled 30 mm from its starting position and returned to its starting position. Fig. 3 shows an Abaqus rendering of the FEM during loading and unloading. In Fig. 3(a), the V-press is displaced by 30 mm, and it can be seen that the plate has bent to an angle of approximately 100°. Fig. 3(b) shows the system once fully unloaded. In this case, it can be seen that the bend angle has increased to 143°, i.e. a significant elastic springback of 43°, which is an undesirable distortion of the metal product. The springback phenomenon is common in metal bending, and is caused by elastic recovery of a material after the bending load has been released [15].

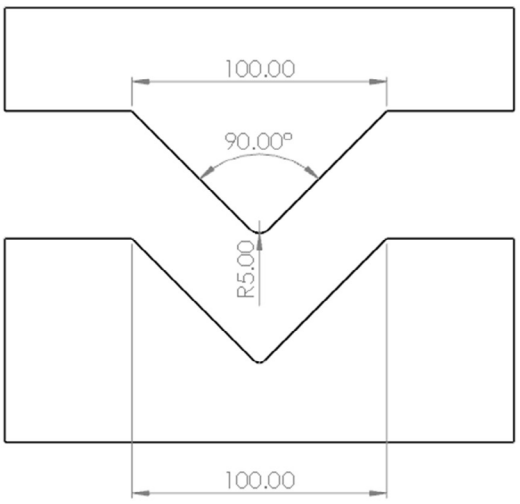

Fig. 2 Schematic showing V-press and die geometry

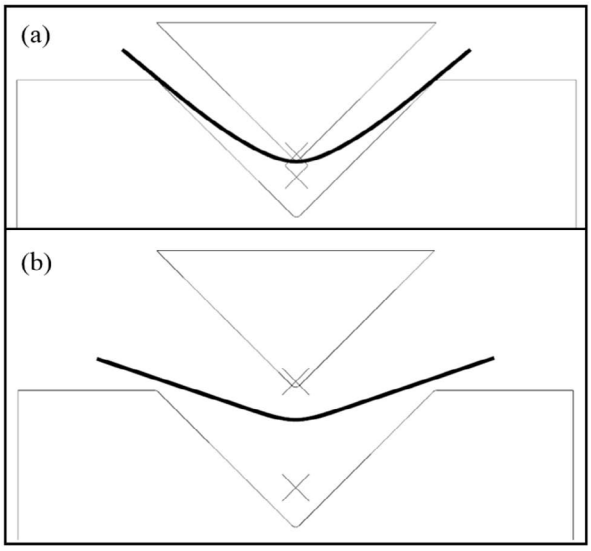

Fig. 3 FEM model showing (a) 30 mm displacement of V-press; (b) retraction of V-press showing elastic recovery of specimen

One of the benefits of the process digital twin is the ability to predict internal stress during bending, as well as residual stress post-bending. Fig. 4 (a) shows the stress distribution in the plate during bending. At the point where the V-press is in contact with the plate, the local compressive stress is approx. 443 MPa, while on the opposite side of the specimen, the workpiece is in a state of tensile stress of 416 MPa. Fig. 4(b) maps the residual stress distribution in the specimen after the V-press has been completely retracted. The largest residual stresses are located nearer to the neutral axis of the specimen. Fig. 5 plots the stress profile across the thickness of the specimen for the loaded and unloaded condition. It can be seen at the edge of the specimen, on the left axis of the graph, the

stress condition changes from 443 MPa compression in the loaded state, to a predicted residual tensile stress of 185 MPa when fully unloaded. The residual stress profile is typical of that seen for a plate under elastic-plastic bending.

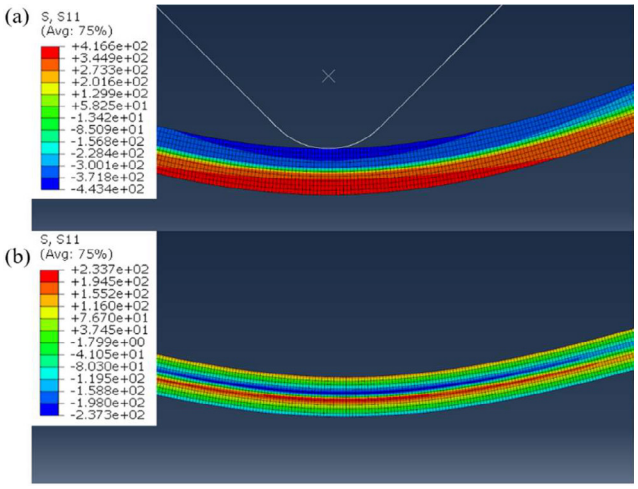

Fig. 4: FEM S11 stress distribution for workpiece when (a) fully loaded with 30 mm V-press displacement and; (b) residual stress distribution after bending load has been removed

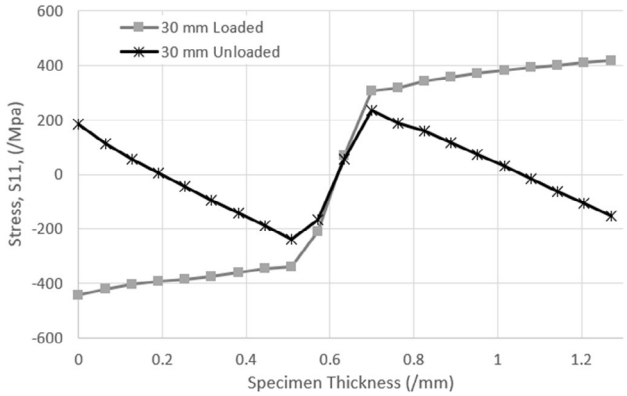

Fig.5 Plot of stress across the thickness of the specimen for fully loaded and unloaded conditions for 30 mm V-press displacement

3.2 Process physical twin: 30 mm displacement

In order to validate the virtual model, a physical bending test was conducted on ten specimens, with a V-press displacement set to 30 mm using the physical bending test bed. Although it was not possible to measure stress during the bending cycle, the final bend angle could be verified against FEM results. Fig. 6 presents a photograph of the ten specimens bent using the 30 mm displacement. A Vernier calipers was used during the bending process to measure the displacement repeatability of +/- 0.2 mm between the V-press and die during physical testing. Post-testing, the final bend angles of all ten specimens were measured, resulting in an average bend angle of 142.58°, with a standard deviation of 0.33°. The modeled angle of 143° is within 2 standard deviations of the physical tests – thus showing good fidelity of the process digital twin with the process physical twin.

3.3 Process digital twin: 45 mm displacement

To further test the validity of the FEM-based process digital twin, a second scenario was tested, this time using a V-press displacement of 45 mm. Fig. 7 shows an Abaqus® rendering of the model in the loaded state (Fig.7(a)) and unloaded state (Fig.7(b)) for the 45 mm V-press displacement. For the loaded condition, the bend angle is 90°, where it can be seen that the sides of the plate are in full contact with the surfaces of the die. Upon unloading however, it is again seen that the material undergoes elastic recovery, resulting in springback of 15.2 ° to an angle of 105.2°.

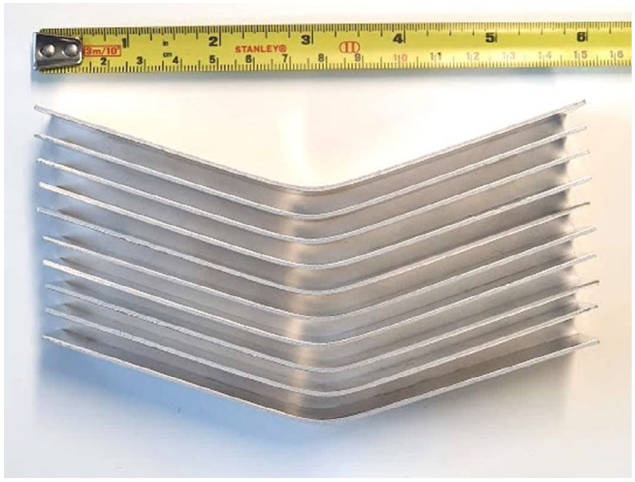

Fig.6 Photograph of ten specimens which were bent to 30 mm displacement.

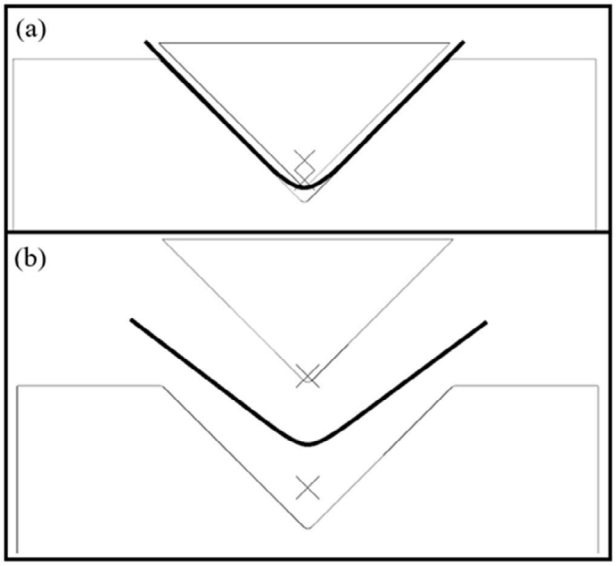

Fig.7 FEM model showing (a) 45 mm displacement of V-press; (b) retraction of V-press showing elastic recovery of specimen

Fig. 8 (a) presents the predicted stress distribution across the metal plate during bending to 45 mm displacement. At the point where the V-press is in contact with the workpiece, the local compressive stress is predicted to be 583 MPa – a considerable increase over the 30 mm FEM. On the opposite side of the specimen, the plate is again in a state of tensile stress, this time to the magnitude of 510 MPa. The predicted residual stress distribution post-bending is presented in Fig.8(b). As expected, the magnitude of predicted residual stress in this specimen type is larger than the 30 mm model. Fig. 9 plots the predicted stress

profile across the thickness of the specimen for the loaded and unloaded condition. In this case, it can be seen at the edge of the specimen, on the left axis of Fig. 9, the stress condition changes from a compressive stress of 583 MPa in the loaded state, to a residual tensile stress of 310 MPa when the V-press is fully retracted from the specimen and elastic recovery has occurred.

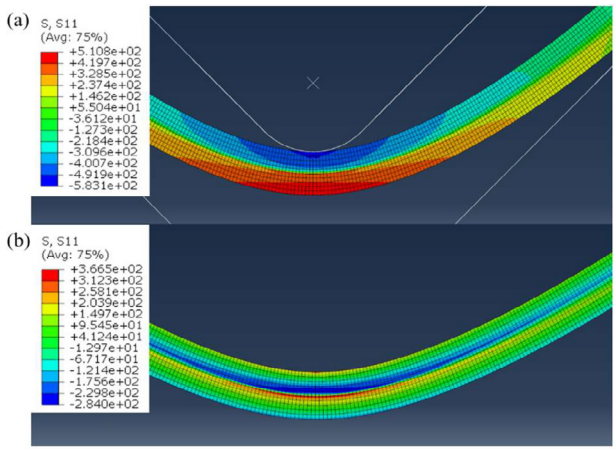

Fig. 8: FEM S11 stress distribution for workpiece when (a) fully loaded with 45 mm V-press displacement and; (b) residual stress distribution after bending load has been removed

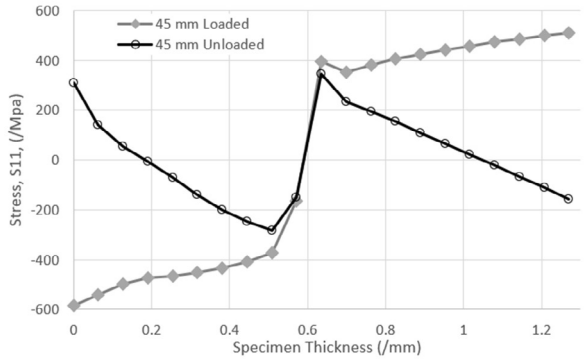

Fig. 9 Plot of stress across the thickness of the specimen for fully loaded and unloaded conditions for 45 mm V-press displacement.

3.4 Process physical twin: 45 mm displacement

To further validate the fidelity of the process digital twin, a second test was conducted using the physical hardware. In this case, ten specimens were bent to a V-press displacement of 45 mm, a photograph of these specimens post-bending is presented in Fig. 10. The average bend angle was calculated to be 108.2°, with a standard deviation of 0.38°. This shows a greater difference between the predicted model and physical specimens compared to the 30 mm bend test, where a difference of 3° was observed – falling beyond seven standard deviations away from the mean.

4. Discussion

Comparing the FEA results from the process digital twin for the 30 mm and the 45 mm displacement models, a notable difference was observed for springback angles. The former model predicted a springback angle of 43°, while the latter model calculated a springback of just 15.2°. This can be explained by examining the bend angles in Fig. 3(a) and Fig. 7(a). In Fig. 3(a), it can be seen that the plate is bowing between the V-press and die. This bowing shape is largely in the elastic region of the material, with limited plastic deformation where the V-press meets the plate. Thus, as the V-press is removed, a large amount of elastic recovery and thus springback is observed. Comparing this to the 45 mm displacement model in Fig. 7(a), it can be seen that the sides of the specimen are pressed flat against the wall of the die, resulting in far less elastic deformation in these regions, but a larger region of plastic deformation around the nose of the V-press. It has been reported for V-bending of aluminium that springback decreases as the area of plastic deformation increases, thus, less springback is expected in the 45 mm displacement model compared to that of the 30 mm displacement model [17].

Additionally, it was observed that the difference between the measured and predicted bend angles is larger for the 45 mm specimens than the 30 mm specimens (3° difference vs. 0.42° difference). As the strain in the 30 mm sample was largely in the elastic zone, it is suggested that the discrepancy for the 45 mm model may be caused by the plastic data used for Al2024 T3, which may not be entirely reliable at large strains. Furthermore, discrepancy may also arise with regard to modelling the frictional effects. It can be seen in Fig 3.(a) that when the press is fully displaced for the 30 mm specimen, the workpiece is only in contact with the outer radii of the die opening. For the 45 mm displacement however, it can be seen in Fig 7.(a) that the workpiece is in contact with the die face for approximately 37 mm on each side. During the bending, the workpiece slides along this die face and thus, the influence of the coefficient of friction between the workpiece and die has a considerably greater effect on the 45 mm bending.

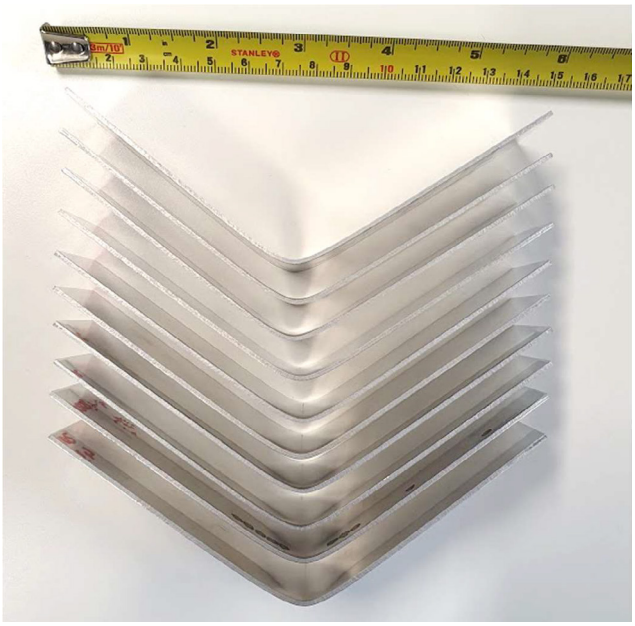

Fig.10 Photograph of ten specimens which were bent to 45 mm displacement.

It is evident from the results that there is good fidelity between the FEM-based process digital twin, and the physical manufacturing process for the bending of aluminium. Having such virtual process models is advantageous for manufacturing industries, especially aerospace and automotive sectors, where aluminium is frequently formed to produce lightweight

components [19]. Not only does this give a manufacturer an insight into how the process will perform, it also provides information about the status of the product after the manufacturing step. For example, a key concept of smart manufacturing is the mass production of customised products [20]. Customised products may require new manufacturing processes using new materials, with unknown consequences of how these materials will perform during the manufacturing operations. Traditionally for metal bending operations, a desired bend angle would be obtained using designer experience, coupled with trial an error [21]. This is both time-consuming and costly for manufacturers [22]. By using a process-based digital twin approach, different manufacturing configurations can be simulated and de-risked, adding value and reducing time to market [19].

In metal forming operations, the process digital twin element can be used to ensure desired results (such as a specific final bend angle). These results can be provided to the machine digital twin to update machine actions, improving manufacturing efficiency. Furthermore, the product digital twin can be updated with the predicted material state such as bend angle and residual stress which can be used to improve subsequent manufacturing steps and product performance. Thus, considering the digital twin with three components: the machine, the product and process, can help optimise business performance using high-fidelity process models.

5. Conclusion and Outlook

This paper highlighted a new approach for manufacturing based digital twin, which consists of three primary elements – the machine, the product and the process. An FEM-based process digital twin is used to predict process performance and outcomes for a V-bending operation. Using a bespoke V-bending test bed, the process digital twin has been validated for two test scenarios.

For a V-press displacement of 30 mm, the predicted final bend angle is 143°, while the average measured physical bend angle is 142.58° with a standard deviation of 0.33°. The maximum stress during bending is calculated to be 443 MPa compression, resulting in a predicted tensile residual stress of 185 MPa once unloaded.

For a V-press displacement of 45 mm, the predicted final bend angle is 105.2°, while the average measured physical bend angle is 108.2° with a standard deviation of 0.38°. Maximum stress during bending is 583 MPa compression, resulting in a predicted tensile residual stress of 310 MPa once unloaded.

While the bend angle was used to experimentally verify the FEA modelling with real-world bending, the residual stress was not experimentally verified, and thus, future work will endeavor to experimentally verify the residual stress within the components post-bending. Additionally, it is planned that FEA data will be used to control the physical manufacturing process to ensure desired product outputs for a range of different materials. For the purpose of this paper, the product was not serialized, however, it is the intention to serialize the metallic strips prior to bending, which will be barcoded and scanned. Thus, a more comprehensive digital-twin based device history record can be developed in future.

Acknowledgements

This publication has emanated from research conducted at the Confirm Smart Manufacturing Centre with the financial support of Science Foundation Ireland (SFI) under Grant Number SFI/16/RC/3918, co-funded by the European Regional Development Fund. EH acknowledges the assistance of Dr David Tanner in the development of the FE models.

Appendix A. Plastic Properties of Al2024 T3 Plate

Fig. A.1 graphs the plastic properties used in the FEA simulations of this paper for Al2024 T3 plate. These values were obtained from [23].

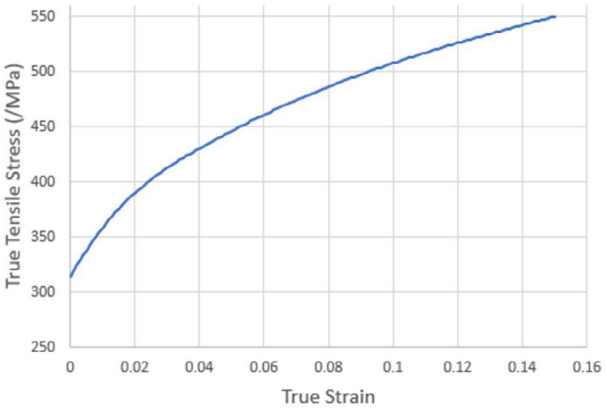

Fig.A.1 Graph plotting true tensile strength vs. true strain for Al2024 T3 plate obtained from [23].

References

[1] H. Lasi, P. Fettke, H.-G. Kemper, T. Feld, and M. Hoffmann, 'Industry 4.0', *Business & information systems engineering*, vol. 6, no. 4, pp. 239–242, 2014.

[2] H. S. Kang *et al.*, 'Smart manufacturing: Past research, present findings, and future directions', *International Journal of Precision Engineering and Manufacturing-Green Technology*, vol. 3, no. 1, pp. 111–128, 2016.

[3] R. Y. Zhong, X. Xu, E. Klotz, and S. T. Newman, 'Intelligent manufacturing in the context of industry 4.0: a review', *Engineering*, vol. 3, no. 5, pp. 616–630, 2017.

[4] P. Wright, 'Cyber-physical product manufacturing', *Manufacturing Letters*, vol. 2, no. 2, pp. 49–53, 2014.

[5] L. Monostori, 'Cyber-physical production systems: Roots, expectations and R&D challenges', *Procedia Cirp*, vol. 17, pp. 9–13, 2014.

[6] Y. Lu, C. Liu, I. Kevin, K. Wang, H. Huang, and X. Xu, 'Digital Twin-driven smart manufacturing: Connotation, reference model, applications and research issues', *Robotics and Computer-Integrated Manufacturing*, vol. 61, p. 101837, 2020.

[7] A. Canedo, 'Industrial IoT lifecycle via digital twins', in *Proceedings of the Eleventh IEEE/ACM/IFIP International Conference on Hardware/Software*

Codesign and System Synthesis, 2016, p. 29.

[8] E. Negri, L. Fumagalli, and M. Macchi, 'A review of the roles of digital twin in cps-based production systems', *Procedia Manufacturing*, vol. 11, pp. 939–948, 2017.

[9] F. Tao, Q. Qi, L. Wang, and A. Y. C. Nee, 'Digital twins and cyber-physical systems toward smart manufacturing and Industry 4.0: Correlation and comparison', *Engineering*, vol. 5, no. 4, pp. 653–661, 2019.

[10] Q. Qi and F. Tao, 'Digital twin and big data towards smart manufacturing and industry 4.0: 360 degree comparison', *Ieee Access*, vol. 6, pp. 3585–3593, 2018.

[11] A. M. Madni, C. C. Madni, and S. D. Lucero, 'Leveraging digital twin technology in model-based systems engineering', *Systems*, vol. 7, no. 1, p. 7, 2019.

[12] B. Scaglioni and G. Ferretti, 'Towards digital twins through object-oriented modelling: a machine tool case study', *IFAC-PapersOnLine*, vol. 51, no. 2, pp. 613–618, 2018.

[13] T. DebRoy, W. Zhang, J. Turner, and S. S. Babu, 'Building digital twins of 3D printing machines', *Scripta Materialia*, vol. 135, pp. 119–124, 2017.

[14] A. Chaudhary, 'Modeling of laser-additive manufacturing processes', *ASM Handbook*, vol. 22, pp. 240–252, 2009.

[15] S. D. El Wakil, *Processes and design for manufacturing*. CRC Press, 2019.

[16] S. Boschert and R. Rosen, 'Digital twin—the simulation aspect', in *Mechatronic Futures*, Springer, 2016, pp. 59–74.

[17] W. M. Chan, H. I. Chew, H. P. Lee, and B. T. Cheok, 'Finite element analysis of spring-back of V-bending sheet metal forming processes', *Journal of materials processing technology*, vol. 148, no. 1, pp. 15–24, 2004.

[18] Y. E. Ling, H. P. Lee, and B. T. Cheok, 'Finite element analysis of springback in L-bending of sheet metal', *Journal of Materials Processing Technology*, vol. 168, no. 2, pp. 296–302, 2005.

[19] V. Esat, H. Darendeliler, and M. I. Gokler, 'Finite element analysis of springback in bending of aluminium sheets', *Materials & design*, vol. 23, no. 2, pp. 223–229, 2002.

[20] M. Brettel, N. Friederichsen, M. Keller, and M. Rosenberg, 'How virtualization, decentralization and network building change the manufacturing landscape: An Industry 4.0 Perspective', *International journal of mechanical, industrial science and engineering*, vol. 8, no. 1, pp. 37–44, 2014.

[21] S. J. Thanki, H. K. Raval, and A. K. Dave, 'Prediction of the punch reversal position under V-plate bending using real material (power-law) behavior', *Journal of Materials Processing Technology*, vol. 114, no. 3, pp. 227–232, 2001.

[22] S. K. Panthi, N. Ramakrishnan, K. K. Pathak, and J. S. Chouhan, 'An analysis of springback in sheet metal bending using finite element method (FEM)', *Journal of Materials Processing Technology*, vol. 186, no. 1–3, pp. 120–124, 2007.

[23] ASM International, 'Atlas of Stress-Strain Curves', in *Atlas of Stress-Strain Curves*, 2nd ed., 2002, p. 331.